How Sentinel-1 timeseries can improve the implementation of conservation programs in Brazil

Antoine Pfefer, Bertrand Ygorra, Frederic Frappart, Gabriela Demarchi, Benjamin Pillot, Julie Subervie, Wigneron J.-P., Thibault Catry

Remote Sensing Applications: Society and Environment 35 (2024) 101241

Contents lists available at ScienceDirect

Remote Sensing Applications: Society and Environment

journal homepage: www.elsevier.com/locate/rsase

How Sentinel-1 timeseries can improve the implementation of conservation programs in Brazil

Antoine Pfefer [a], Bertrand Ygorra [b], Frederic Frappart [b], Gabriela Demarchi [c], Benjamin Pillot [a], Julie Subervie [c], Jean-Pierre Wigneron [b], Thibault Catry [a, *]

[a] Espace Dev, Univ Montpellier, IRD, Univ Antilles, Univ Guyane, Univ Réunion, Montpellier, France
[b] INRAE, ISPA, Bordeaux Sciences Agro, Villenave D'Ornon, France
[c] CEE-M, INRAE, Montpellier, France

ARTICLE INFO

Keywords:
Deforestation
Conservation
Brazil
Sentinel-1
SAR

ABSTRACT

Cumulative Sum (CuSum) change detection was applied on a Sentinel-1 backscatter time series at a spatial scale of 10 m as part of a conservation program implemented in Acre, Brazil, requiring the monitoring of deforestation activities by participants in the program. This study evaluated the results of CuSum and compared them to those obtained from conventional deforestation products, demonstrating how this method can improve the implementation of such programs. We aimed to map deforestation events with a minimum resolution of 0.1 ha to maximise event detection while minimising false positives, which could lead to unfair penalties for participants. The remarkable detection precision (ranging from 87.3 % to 96.1 %) and short delay of the CuSum algorithm make it suitable for implementing a conservation program, as illustrated in this study. Moreover, this method has the potential to accurately assess the extent of future deforestation. This study contributes to the development of effective deforestation monitoring strategies within the framework of conservation programmes to facilitate improved farming practices and climate change mitigation. This code is available at https://github.com/Pfefer/cusum.

1. Introduction

Deforestation of tropical rainforests is a major issue for biodiversity conservation, the terrestrial carbon cycle, indigenous population subsistence, and, more generally, in the broader fight against deforestation to help mitigate climate change (Gibson et al., 2011; Gatti et al., 2021). In 2012, smallholders owned 24 % of the Brazilian Legal Amazon. Their plots of areas less than 100 ha represented 12 % of the total deforestation (Godar et al., 2014; Maurano and Escada, 2019; Trancoso, 2021). Tyukavina et al. (2018) showed the major contribution of smallholders to the dynamics of deforestation. Kalamandeen et al. (2018) reported that the average size of forest-loss patches in the Amazon between 2001 and 2014 was 10.25 ha. This study also highlighted that the majority (96.4 %) of deforested patches in the Amazon were below the 6.25-ha threshold set by Prodes (Almeida et al., 2021), with a significant proportion of deforested patches (81.1 %) below 1 ha on surface. Trancoso (2021) reported that the average size of deforestation patches in the Brazilian Amazon increased from 10.6 to 24.7 ha in the period 2015–2019 and remained 24.1 ha in 2020. In our specific region, where small-scale farmers represent the majority of landowners, we observed that 87.3 % of deforested areas were smaller than 5 ha (Table 1).

* Corresponding author.IRD/Espace-Dev, Maison de la Teledetection, 500 rue JF Breton, 34093, Montpellier, France.
E-mail address: thibault.catry@ird.fr (T. Catry).

https://doi.org/10.1016/j.rsase.2024.101241
Received 12 March 2024; Received in revised form 3 May 2024; Accepted 8 May 2024
Available online 11 May 2024

Table 1
Distribution of validation polygons area.

Area (Ha)	Polygons (Pol) on extended area	Polygons (Pol) on plots
≤0.2	41 (4.4%)	26 (9.4%)
0.2 < Pol ≤0.5	93 (10.0%)	34 (12.3%)
0.5 < Pol ≤1	167 (18.0%)	167 (18.0%)
1 < Pol ≤5	507 (54.9%)	151 (54.5%)
5 < Pol ≤10	88 (9.5%)	15 (5.4%)
10 < Pol	41 (4.4%)	6 (2.2%)
Total	923	27

Conservation programs promote sustainable practices that contribute to the preservation of natural resources and ecosystems. For several years, programs that offer payments for environmental services (PES) to landowners who agree to conserve their forests have been envisaged as a possible means of combating deforestation resulting from activities such as forestry, cropland expansion, and pasture area expansion on plots owned by smallholders (Montero-de Oliveira et al., 2023). This is particularly the case in Brazil, where there has been a proliferation of sub-national initiatives financed by the Reducing Emissions from Deforestation and Forest Degradation (REDD+) mechanism in the Amazon in recent years (Sills et al., 2014) with more than 50 REDD + projects targeting smallholder farmers (Simonet et al., 2015). We implemented a conservation program in the state of Acre, Brazil, offering PES contracts to 459 smallholders over a one-year period, spanning from June 2021 to December 2021 and continuing until June 2022 to December 2022. The program proposed different payment contracts for smallholders, all of which financially compensated for the preservation of the forest surface over their fields. The main objective was to monitor the state of the forests with maximum precision (ratio between true detected patches of deforestation and the entire set of deforested patches) and minimal delay, to assess the impact of the program on forest conservation. Precision was crucial because patches falsely detected as deforestation areas could lead to unfair financial penalties. The monitoring process aimed to accurately identify and track deforestation activities to ensure compliance with the program guidelines.

Some studies have used publicly accessible resources to monitor deforestation and evaluate the effects of conservation programs (Demarchi et al., 2023). West et al. (2020) employed the MapBiomas dataset (Souza and Azevedo, 2017), while Roopsind et al. (2019) used the Global Forest Watch (GFW) tree cover loss dataset (Hansen et al., 2013). The use of the Prodes (Almeida et al., 2021) and GFW datasets revealed a discrepancy in outcomes, as demonstrated by Demarchi et al. (2023). Several optical products, such as TMF (Tropical Moist Forest, Vancutsem et al., 2021), known for their effectiveness and widespread use, presented issues such as incompatible definitions of primary forest compared to the contractual definition or limitations in the frequency of result publications. For instance, some contracts ended in September 2022, yet TMF and GFW have not published their 2022 data as of April 2023, and TMF data for 2022 are available with a delay of five months (published in May 2023).

In this context, we tested the potential of a recently developed approach based on the cumulative sum (CuSum) technique (Manogaran and Lopez, 2018) applied to the time series of Sentinel-1 backscatter images (Ygorra et al., 2021a). A key advantage of radar-based methods is the regular availability of data, typically every 6–12 d with Sentinel-1, regardless of cloud cover. This method has been previously employed in the Congo for small-scale deforestation and degradation (Ygorra et al., 2021a; and b). Some studies like Doblas Prieto et al. (2023) also demonstrated the complementarity between optical and SAR (Synthetic Aperture Radar) methods for deforestation monitoring in the Amazon. Our primary objective was to monitor deforestation activities among PES program participants to assess the effectiveness and impact of the program. In addition, we conducted a test of the CuSum algorithm in a nearby zone ("extended area", Fig. 1) covering an area of 150,000 ha to assess the algorithm performance specifically within the timeframe of October 2020 to October 2021, allowing for a comparison of its results with those obtained from other available products.

2. Methodological approach

2.1. Study sites

The study sites encompassed two areas: plots of the PES program, covering a total area of 26,000 ha (as defined by Demarchi, 2022), and a nearby testing zone "extended area" located in the state of Acre, Brazil (Fig. 1). The climate in these areas is characterised as warm and humid, with an average annual temperature of 25 °C and mean annual rainfall ranging from 2000 to 2500 mm.

2.2. Datasets

2.2.1. Sentinel-1 SAR images

The Sentinel-1 mission is a constellation of two satellites positioned at an altitude of 693 km, with a 180° orbital phasing difference (Torres et al., 2012). Each satellite has a repeat cycle of 12 days over the study site. Sentinel-1A and B were launched in April 2014 and April 2016, respectively. The instrument onboard the Sentinel-1 satellite was a C-band Synthetic Aperture Radar (SAR). In this study, Ground Range Detected products were acquired in the Interferometric Wide-swath mode with a resolution of 5 × 20 m resampled to 10 × 10 m, using vertical-vertical (VV) and vertical-horizontal (VH) polarisations. Data from the Sentinel-1A (ascending) and B (descending) satellites were used in our analysis, covering a total of 60 images captured between October 31, 2020 and October 31, 2021.

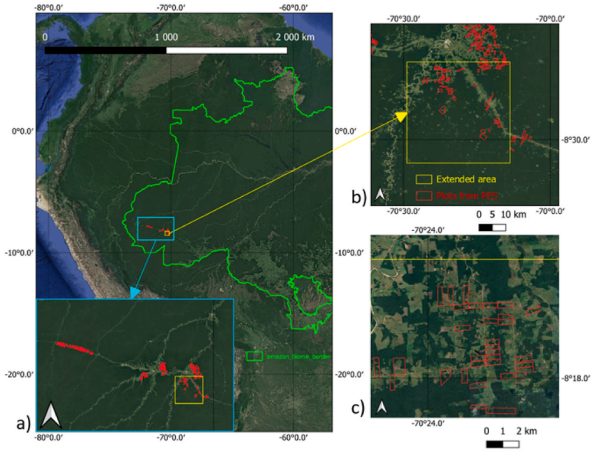

Fig. 1. a) Study site located in Amazonia, in the Brazilian state of Acre. b) and c) Plots from PES are in red and the "extended area" on which we assessed the performance of the algorithm is in yellow. (For interpretation of the references to colour in this figure legend, the reader is referred to the Web version of this article.)

2.2.2. PlanetScope optical images

PlanetScope monthly mosaics provided by the NICFI program (Roy et al., 2021) were used to manually delineate the deforestation polygons (Fig. 2). These images have a high resolution of 4.77 m and minimal cloud coverage. By comparing the images of October 2020 with those of October 2021, 928 deforested polygons were identified manually and digitised, covering a total area of 2950 ha.

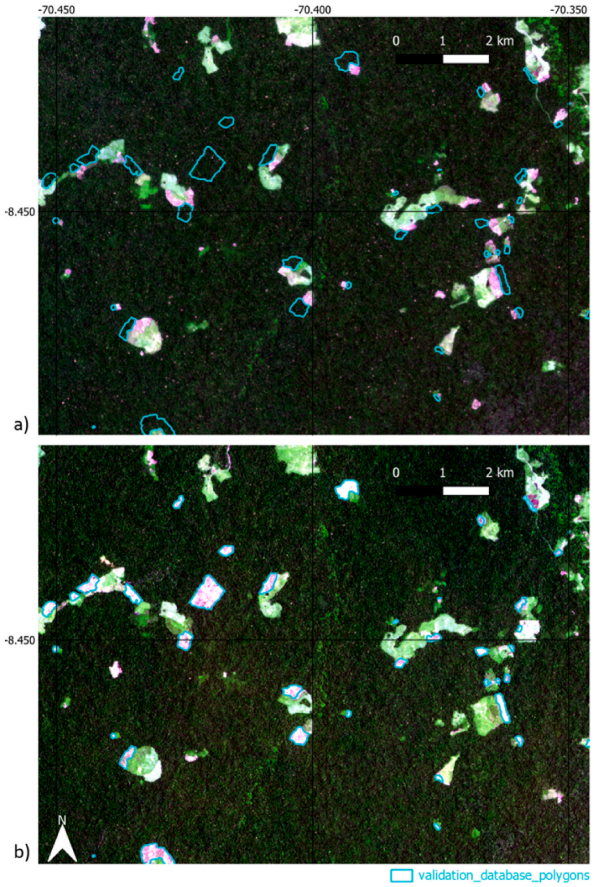

Fig. 2. a) Sample of the study site on October 2020 PlanetScope image. b) Same sample on October 2021 PlanetScope image. Blue polygons are the validation database polygons hand-drawn. Imagery © 2021 Planet Labs Inc. (For interpretation of the references to colour in this figure legend, the reader is referred to the Web version of this article.)

This visual interpretation was combined and validated using the expertise of local partners who conducted field surveys directly related to program implementation.

2.2.3. Tropical Moist Forest mask

To delineate the study area and exclude potential algorithm detections within non-forested areas, we used the TMF deforestation monitoring results from 1982 to 2020 as a non-forest mask. The initial comparison between the masks in the TMF and GFW groups revealed no significant differences. However, we chose this specific mask because of its definition of degradation, which could enhance the detection of disturbance events, resulting in a higher identification of non-forest spaces.

2.2.4. Available and existing deforestation products

CuSum was compared to classical and state-of-the-art deforestation products: GFW, TMF, GLAD-S2 (Pickens et al., 2020), Brazilian-specific Prodes, and MapBiomas. RAdar for Detecting Deforestation (RADD, Reiche et al., 2021) was also used as a reference for comparison because, like CuSum, it employs an approach based on the analysis of the Sentinel-1 time series. Only products in Brazil that provided free and readily downloadable data were included in this study. The GFW provides an annual map of tree cover loss, starting in 2000. It is based on the analysis of the Landsat reflectance at 30 × 30 m using a decision-tree algorithm. The product is updated annually to provide information on deforestation and land cover changes. The TMF is another optical product based on a decision algorithm applied to Landsat data to identify deforested areas. The TMF distinguishes between deforestation, which refers to disturbances visible for over 2.5 years, and degradation, which represents deforestation visible for less than 2.5 years. Prodes is a deforestation monitoring system that relies on photo-interpretation. It specifically identifies point deforestation events with an area greater than 6.25 ha within a predefined period from August 1st to July 31st each year. MapBiomas employs machine-learning algorithms to automatically identify patterns and changes associated with deforestation, allowing for accurate detection and monitoring of deforestation activities. These optical products provide valuable insights into deforestation, but may have limitations in terms of cloud cover and timeliness of data availability. RADD uses Sentinel-1 data and analyzes backscatter information using a probabilistic algorithm to detect and identify deforestation activities. By leveraging radar backscatter data, RADD can overcome some of the limitations associated with cloud cover and obtain more consistent and frequent observations than optical-based methods. TropiSCO (Bouvet et al., 2018) and DETER-R (Doblas et al., 2022) also used Sentinel 1 data to identify deforestation; however, the data for Brazil are not freely available (TropiSCO) or readily downloadable (DETER-R, only providing access to the code).

2.3. Method

The entire package for executing the algorithm is available at https://github. com/pfefer/cusum.

2.3.1. Sentinel-1 data pre-processing

Sentinel-1 data were downloaded from the SNAP API and preprocessed using the PyroSAR (Truckenbrodt et al., 2019) and PyRAT (Reigber et al., 2019) packages. The preprocessing steps included orbital correction, thermal noise correction, border noise correction, terrain correction, radiometric calibration to sigma naught, and bilateral speckle filtering using a 3 3 window, as outlined by Ygorra et al. (2021a, Fig. 3).

2.3.2. CuSum algorithm

The algorithm analyzes the time-series backscatter values for both the VV and VH polarisations at the pixel scale. It detects changes by computing the cumulative sum of the difference between the backscatter signal and its mean over a given period of N images (Ygorra et al., 2021a). This cumulative sum analysis helped identify significant changes in backscatter values, indicating potential deforestation events.

$$R_k = \sum_{i=1}^{k} R_{i,j}$$

where $k \in \{1, ..., N\}$, $R_{i,j} = \gamma_{i,j} - \sigma_j$.

$\gamma_{i,j}$ backscatter signal value from pixel j at time i and σ_j the time average of the signal on the pixel j.

Then we compute the amplitude:

$$A_j = max\ R_k - \min\ R_k \text{ with } k \in \{1, .., N\}$$

We then implemented a bootstrapping step to randomise our initial time series 500 times. This randomisation process involves shuffling the order of the backscatter values within the time series. We chose 500 after previous tests, as described by Ygorra et al. (2021a). Moreover, we computed the new amplitude, Ar, for each randomisation. Finally, we compute the ratio CL (Confidence Level) between the number of randomisation which have an amplitude Ar ≤ Ai the total number of randomisation (500):

$$CL = \frac{\left|\left\{A_r \le A_i, \mathrm{r} \in \left\{1, ..., 500\right\}\right\}\right|}{500} \quad (1)$$

We introduce a threshold Tc used to accept a change when CL ≥ Tc. The Tc threshold value is an adjustable parameter that users can customise. These steps are performed for each pixel j.

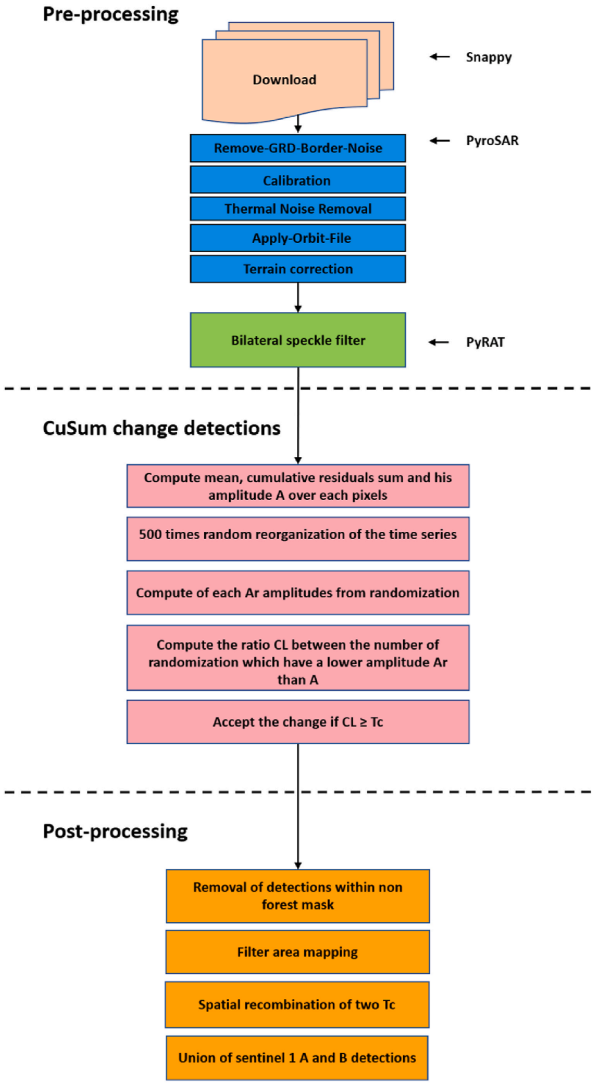

Fig. 3. Flowchart illustrating the three main steps of the radar-based deforestation monitoring method: pre-processing, CuSum algorithm change detection, and post-processing.

2.3.3. Post-processing

In the post-processing steps, several measures were taken to improve the accuracy and reliability of the algorithm outputs. i) Non-forest mask: the algorithm removed any detections within a non-forest mask, defined using the TMF deforestation results from 1982 to early 2020. ii) Removal of previous detections: The algorithm was run for an earlier time period (October 2020 for the testing zone and until June 2021 for the plot study), and any detections that were already identified in the previous run were removed. This step ensured that only new and recent deforestation events were considered. iii) Minimum detection size: to minimise false detections, detections smaller than 0.1 ha (10 pixels) are removed. This threshold was chosen in accordance with our primary goal of accurately assessing the extent of deforestation while avoiding false detections that could unfairly penalise participating stakeholders. This threshold aligns with most other deforestation products, thereby enhancing the robustness of our comparison. iv) Spatial recombination: Spatial recombination is applied to the algorithm outputs using two different thresholds, referred to as high and low Tc (Ygorra et al., 2021a). Polygons from the low-Tc output are retained only if they intersect (regardless of the size of the intersection) with a polygon from the high-Tc output. This step allows for an increase in the detection size while maintaining spatial precision, ensuring that the resulting polygons are larger but still reliable. In all analyses, we used 1 for High Tc and varied the low Tc. v) For the "extended area", the algorithm is applied separately to the outputs from both Sentinel-1A and B, and the spatial union of the two outputs is obtained.

2.3.4. Validation steps

A reference map was created by comparing October 2020 and October 2021 PlanetScope images. The TMF and Hansen datasets helped to distinguish between primary and secondary forests. Only completely cleared primary forest regions were manually outlined to establish a reference map. In the context of our PES program, an analysis was conducted using PlanetScope images from the start

and end of the contract dates to identify primary forest cuts within the participants' plots. Table 1 shows that most of the events targeted for detection had an area ranging from 1 ha to 5 ha, indicating the size distribution of the detected forest cuts.

2.3.5. Evaluation of algorithm performance

The algorithm performance was evaluated from October 2020 to October 2021. This decision was mainly motivated by the PES contractual agreements that mainly took place during this period. Despite temporal discrepancies in data sources such as MapBiomas or Prodes (July to July period), the use of the October to October period should not have a significant impact on the validity of the comparison in this area, as this period encompasses the main deforestation activities in our region according to i) stakeholder declaration, during which farmers indicated their customary practice of forest cutting exclusively during the dry season, and ii) the deforestation period (from May to November in 2021, April to November in 2022) highlighted by the results from ScienceForAmazonas (2022) in our study area. Moreover, this approach excludes deforestation monitoring during the rainy season. By doing so, we effectively reduced the length of the time series from 60 to 36 images per year, minimising the computation time and the risk of speckles in the Sentinel-1 images caused by rainy conditions, resulting in a higher likelihood of false detections (Ygorra et al., 2021a). We adopted the definition of primary forest outlined by the National Institute for Space Research (INPE) in their Prodes methodology publication (Almeida et al., 2021). Our focus on the primary forest aligned with the requirements specified in the PES contracts, thus ensuring consistency between our analysis and the program objectives. Furthermore, our main emphasis was on deforestation, which is defined as the complete removal of visible canopy cover at the pixel scale.

We used the same three statistical indicators as in (Ygorra et al., 2021a) to assess the algorithm performance:

$$\bullet\ Accuracy = \frac{TP + TN}{TP + TN + FP + FN}$$

The overall Accuracy measures the algorithm ability to correctly classify both "cover change" and "no cover change" pixels. True Positives are the pixels correctly classified as "cover change" by both the reference map and the algorithm. True Negatives are pixels correctly classified as "no cover change" by both the reference map and the algorithm. False Positives (FP) represent the pixels that are incorrectly classified as "cover change" by the algorithm but not by the reference map. False Negatives are the pixels that are incorrectly classified as "no cover change" by the algorithm but identified as "cover change" by the reference map.

$$\bullet Precision = \frac{TP}{TP + FP}$$

Precision measures an algorithm's accuracy in correctly identifying pixels as "cover change" among all the pixels it classified as such. Precision provides insights on the algorithm ability to avoid false positives and is particularly useful when minimising the number of incorrect "cover change" classifications is important.

$$\bullet Recall = \frac{TP}{TP + FN}$$

Recall evaluates an algorithm's ability to correctly identify pixels that are classified as "cover change" by the reference map. The Recall provides insights into the algorithm ability to capture all instances of "cover change" and is particularly useful when the detection of positive cases is of high importance.

To minimise false detections and accurately assess deforestation areas, we focused on maximising precision (the ratio of correctly detected deforestation pixels to all detected deforestation pixels) while maintaining satisfactory recall (the ratio of correctly detected deforestation pixels to all actual deforestation pixels) at the pixel scale. In addition, we compute a metric on a polygon scale. This metric calculates the ratio between the number of reference map polygons successfully detected by the algorithm and the total number of reference map polygons, regardless of the size of the detection. This metric allowed us to measure the portion of reference polygons detected by the algorithm without considering the precision of the detection size.

$$\bullet Detected = \frac{|\{\mathrm{Pol} | \mathrm{Pol} \cap \mathrm{Algorithm\ Detection}, \emptyset\}|}{|\{\mathrm{Pol}\}|}$$

The detected metric is calculated as the ratio between the number of polygons (Pol) from the validation database that have a non-empty intersection with the algorithm detection and the total number of polygons in the validation database. This metric assesses how well the algorithm identifies polygons representing deforestation events in the study area.

2.3.6. Identification of false positive areas using buffers

To identify FP locations in our algorithm evaluation, we expanded the polygons from the validation dataset with 10 m, 20 m, and 60 m buffer zones and computed the metrics over these different validation databases.

3. Results

3.1. CuSum overall performances

Cusum algorithm is able to detect 86.1 % of the identified deforested polygons and achieved 98.9 % accuracy, 87.3 % precision, and 53.2 % recall. An overview (Fig. 4) of results shows how false detection is limited or located along the boundaries of true detec-

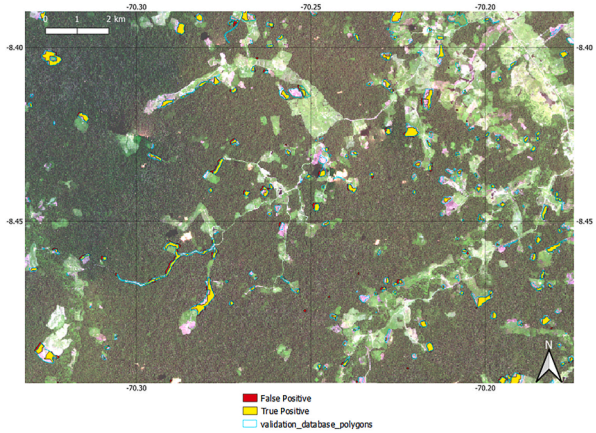

Fig. 4. Results from the algorithm over a sample of the extended area on the October 2021 PlanetScope image; in red is the false positive, and in yellow is the true positive. © 2021 Planet Labs Inc. (For interpretation of the references to colour in this figure legend, the reader is referred to the Web version of this article.)

tion (see Discussion). We can obtain a better recall by decreasing the low Tc (Table 2), but at the expense of increasing false detections.

3.2. Change detection time lags

To determine the time lag in detection using the CuSum algorithm, we selected deforestation events that visually occurred between two cloud-free Sentinel-2 images captured five days apart, providing a 5 days range during which these events occurred. Using different sets of recent Sentinel-1 images as input, our tests showed that to identify an event at time T, the algorithm required four to five subsequent images representing 48–60 d. Furthermore, this result for the detection latency stems from the spatial recombination of Tc 100 and Tc 95. By exploring different combinations, it is possible to reduce the latency to three images while achieving optimal performance (Ygorra et al., 2023). This time lag can be explained by the inherent lag of the cusum because the time series of the sum of the residuals is always zero at the end over pixel j:

$$R_k = \sum_{i=1}^{k} R_{i,j}$$

$$=> \; R_N = \sum_{i=1}^{N} R_{i,j} = \sum_{i=1}^{N} \gamma_{i,j} - \sigma_j = \sum_{i=1}^{N} \gamma_{i,j} - N\sigma_j$$

$$=> \; R_N = \sum_{i=1}^{N} \gamma_{i,j} - N\frac{\sum_{i=1}^{N} \gamma_{i,j}}{N} = 0$$

This implies that if the backscatter time series shows a drop towards the end, the residual remains at 0, regardless of whether a drop occurs. This makes it difficult to observe changes when counting amplitudes below a set threshold. In fact, the smaller the original amplitude, the lower is the probability of obtaining a lower amplitude through bootstrap reorganisation. As a result, even a drop in the backscatter at the end of the series would remain undetected. Additionally, backscatter is influenced by two primary factors, roughness and dielectric properties, which, in turn, can be influenced by moisture (vegetation water content in dense canopies, soil moisture over recently deforested areas, and a combination of the two for low-density canopies and lower vegetation). Following a forest cut, there may be instances in which tree trunks or branches are left behind, and changes in humidity levels can cause an increase in backscatter beyond the initial value observed over a forest pixel. Depending on the case, a double bounce can induce an in-

Table 2
Results for different Tc_low outputs.

Tc_low	Accuracy	Precision	Recall	Detected
97	98.83	88.5	45.8	85.1
96	98.86	87.8	49.5	85.5
95	98.94	87.3	53.2	86.1
94	98.87	80.6	55.3	86.2
93	98.86	78.1	57.3	86.9
91	98.79	72.0	61.1	87.0
89	98.66	65.6	65.2	87.5
87	98.47	59.0	69.1	87.7

crease in backscatter, whereas high moisture and low roughness result in a decrease in backscatter. However, it is only after a certain delay, once the moisture levels stabilize, that a drop in the backscatter time series may occur.

3.3. Comparison between products

A preliminary experiment in the study area revealed that eliminating the wet season resulted in a 19 % increase in precision (which is the most significant objective for us) and a decrease by 3.8 % in polygon detection. This suggests that, although removal is significantly effective for precision, it prevents us from detecting some of the cuts that occurred during this period. Therefore, if we have results from the TMF for 2021 from January to December, we expect them to accurately represent our time period from October 202 to October 2021, October 2020 to April 2021, and October 2021 to December 2021, and few deforestation events should occur. Several annual and near-real-time deforestation products were evaluated during the testing period from October 2020 to October 2021 (Fig. 5).

CuSum achieved an accuracy of 0.989, which was comparable to the accuracy scores of GFW (0.990) and TMF (0.989). This indicated a high level of overall prediction accuracy. In terms of precision, CuSum was the top performer, with a score of 0.873, demonstrating its remarkable ability to accurately identify true-positive results. GLAD-S2 followed closely, with a precision score of 0.842, whereas RADD achieved a precision of 0.799. The remaining products exhibited lower precision. The GFW obtained the highest recall score of 0.847, indicating a high sensitivity level in the detection of relevant data. GLAD-S2 achieved a recall score of 0.699, and CuSum and RADD trailed slightly behind with scores of 0.532 and 0.522, respectively. In terms of the detection rate, GFW outperformed with a rate of 0.957. TMF and RADD performed similarly with rates of 0.926 and 0.929, respectively (Table 3).

CuSum achieved a detection rate of 0.861, indicating satisfactory performance. A comparison of the results of the two radar-based deforestation products (CuSum and RADD) revealed notable similarity (Fig. 6). However, it is important to highlight that RADD demonstrates a higher overall detection rate than the validation database polygons as well as more false positives.

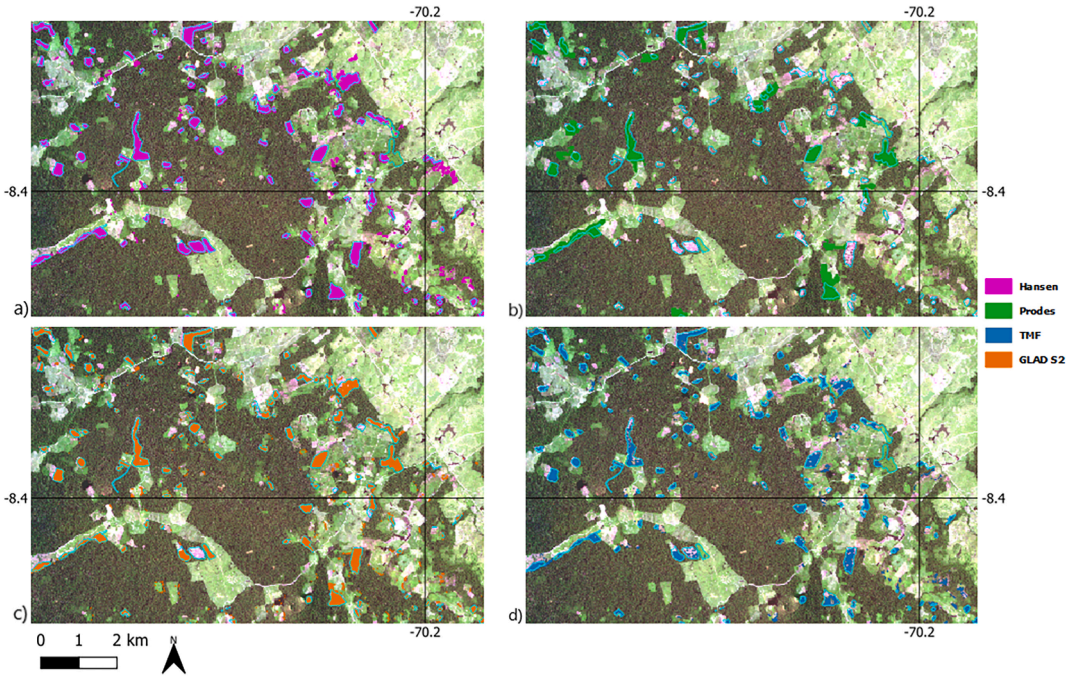

Fig. 5. Results of change detection from other deforestation products: a) GFW, b) Prodes c) GLAD-S2, d) TMF on October 2021 PlanetScope image. Imagery © 2021 Planet Labs Inc.

Table 3
Metrics (%) from different products on extended area between October 2020 and October 2021 computed over the reference dataset (see section 4.2 and Fig. 2). RADD results have been extracted from their highest-level confidence for detections.

Metrics	Hansen	MapBiomas	TMF	RADD	Prodes	GLAD-S2	CuSum
Accuracy	99.0	97.7	98.9	98.8	97.9	99.1	98.9
Precision	72.1	40.3	77.3	79.9	45.1	84.2	87.3
Recall	84.7	34.0	63.7	52.2	32.9	69.9	53.2
Detected	95.7	49.2	92.6	92.9	20.9	90.6	86.1

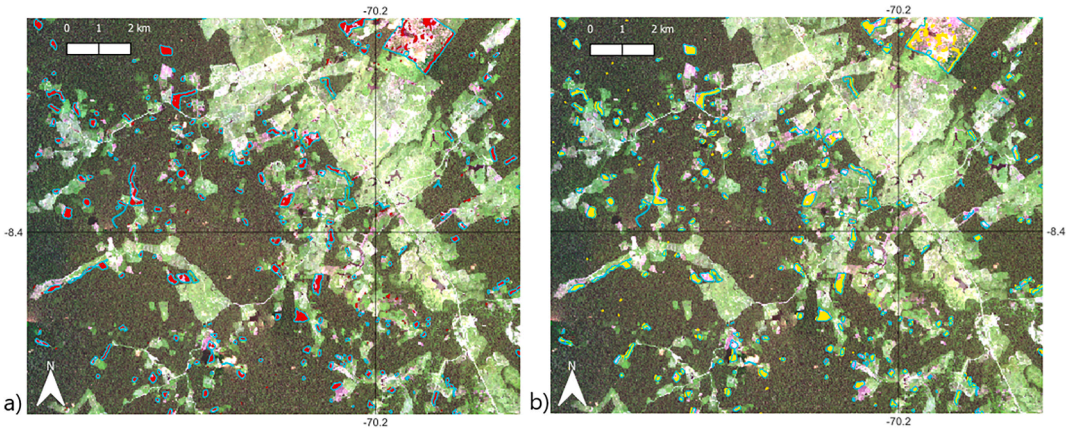

Fig. 6. Results of change detection from RADD in red (a) and CuSum in yellow (b) on October 2021 PlanetScope image. Imagery © 2021 Planet Labs Inc. (For interpretation of the references to colour in this figure legend, the reader is referred to the Web version of this article.)

3.4. Results over the 459 plots in the program

The program was conducted as a randomised controlled trial in 459 households, 302 of which were offered a one-year PES contract. We observed that tree cover declined by 0.74 Ha in treated farm holds during the contract duration (June to October 2022), compared to 1.2 Ha in control farm holds, indicating a 40 % reduction in deforestation (Fig. 7).

4. Discussion

This section discusses the results and the main limitations of the approach with respect to (i) false-positive detections (role of shadows and photointerpretation bias), (ii) false-negative detections (role of the forest/non-forest mask), and (iii) data availability.

4.1. Identification of false positives areas

Computation of the metrics over the buffer dataset showed that 40.7 % of FPs were within 10 m of a validation polygon, 57 % were within 20 m, and 75 % were within 60 m (Table 4).

This suggests that only a few FPs have been isolated from real deforestation. The CuSum algorithm produced more contour errors than pure false deforestation (Table 5). This is a limitation of the study due to bias in digitised validation polygons caused by i) misinterpreting shadows as forested areas during photo interpretation, ii) misinterpretation before/after due to different image capture an-

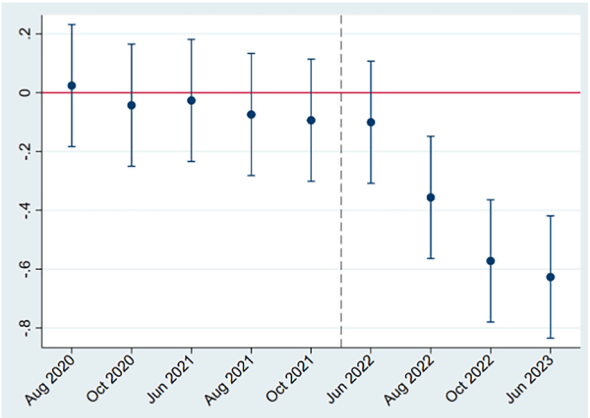

Fig. 7. Impact of the PES program on avoided deforestation. Brackets represent 95 percent confidence intervals. The PES program was implemented at the end of 2021 (dashed line).

Table 4
This table displays the occurrence of false positives over four datasets: the validation database, the validation database expanded by 10 m, 20 m and 60 m.

	Polygons	Polygons +10 m	Polygons +20 m	Polygons +60 m
Area (Ha)	230.58	136.7	99.04	57.67
Precision	87.3	92.5	94.64	96.12
Tendency (%)		−40.7	−57.04	−74.99

Table 5
False positives categorised by type. Boundary +60 represents false positives within the polygons from the validation database buffed by 60 m.

Type FP	Boundary +60 m	Seasonal flooding	Secondary forest	Isolated FP
proportion (%)	74.99	2.23	3.89	18.89

gles, iii) visual canopies not always indicating trees at the pixel scale, and iv) the influence of speckle filtering on clear-cut area boundaries using a 3 × 3 windowing approach. Combining Cusum with a radar shadow detection algorithm, such as that proposed by Bouvet et al. (2018), could help reduce the bias arising from shadow misinterpretation. In addition to this type of false positives, we noticed false detections near to rivers (2.23 %, Fig. 5). Floods can cause changes in the backscatter levels, leading to false-positive changes in the floodplain. In the future, this type of false positives could be avoided by incorporating floodplain areas into non-forest masks. The algorithm is based on spotting changes in the backscatter time series, regardless of the nature of the change. This approach typically detects the secondary forest clearance. However, differentiating it from primary forest clearings and excluding detections within the no-forest mask is crucial to ensure the accurate recognition of primary forest removal. However, incomplete coverage of secondary forest areas in the non-forest mask led to some false positives (3.89 %). Moreover, false positives occurred in primary forests too (18.95 %). This is likely due to backscatter variations from natural factors or misclassifications during the reference map production. For instance, rapid opening and closing of the canopy within the core of primary forests can trigger these issues. Such small-case events can result in subtle canopy cover changes that are not easily visible when comparing images taken one year apart.

4.2. False-negative identification

We addressed the impact of false negatives due to the use of non-forest masks as input, which unintentionally remove deforestation detections in non-forest areas. Our study demonstrates that the delineation of mask edges can lead to misclassification. By intersecting polygon database with the forest mask, false negatives decreased by 36 %, emphasising the need to have an accurate non-forest mask for more reliable deforestation monitoring. Determining the correct balance between filtering non-deforestation changes and accurately detecting deforestation is a challenge in algorithm-based monitoring systems. While it is crucial to remove detections that are not directly related to deforestation, this approach can inadvertently lead to the underdetection of actual deforestation events. This study emphasises the importance of accurate non-forest mask inputs.

4.3. Lack of Sentinel-1 B

The union of ascending and descending Sentinel-1 data played a significant role in achieving notable results. Table 6 shows an improvement in recall and the ratio of detected polygons, increasing by 9 % and 6 %, respectively, with only a 4 % decrease in precision.

However, Sentinel-1B data are no longer accessible, thus imposing limitations. Nevertheless, it is worth mentioning that employing data from a single direction, such as Sentinel 1 A, yielded favourable outcomes at our study sites.

5. Conclusions

We demonstrated the contribution of the CuSum algorithm within the context of a program for environmental services that requires the capability to detect small-scale deforestation, while maintaining accurate estimations of deforested areas to ensure a thorough program evaluation. This method was also compared with various products, the use of which was challenging for this mission because of data inaccessibility, delayed publication of results, different class definitions, and the minimum resolution being too high for our specific case. CuSum demonstrated a global accuracy, detection precision, and recall of 98.9 %, 87.3 %, and 53.2 %, respectively. We updated, developed, and optimised the algorithm to achieve the best performance in monitoring deforestation with minimal false detections, lag, and computational time. By monitoring the deforestation activities of the conservation program participants and conducting tests in a nearby zone, we provided data to assess the effectiveness and impact of the program. This analysis contributes to a better understanding of the capabilities and limitations of the different methods in practical applications within this specific context. The use of radar-based methods such as the CuSum algorithm shows promise for providing timely and accurate information for deforestation monitoring at the local scale. One notable advantage of the CuSum algorithm is its ability to minimise false positives, which is a key issue in conservation programs in which smallholders are paid to preserve primary forests. Additionally, it is a configurable algorithm that allows users to set parameters, such as the minimum mapping unit and Tc combination, giving them the flexibility to prioritise either the number of detections and their associated areas or the precision of the detections.

Table 6
Results from Ascending direction data in input, Descending direction data and Union of both.

	Ascending	Descending	Union of both
Accuracy	98.7	98.8	98.9
Precision	89.9	91.8	87.3
Recall	42.9	44.3	53.2
Detected	77.5	80.2	86.1

Ethical Statement

Hereby, I Antoine Pfefer consciously assure that for the manuscript "How Sentinel-1 timeseries can help improving the implementation of conservation programs in Brazil" the following is fulfilled.

1) This material is the authors' own original work, which has not been previously published elsewhere.
2) The paper is not currently being considered for publication elsewhere.
3) The paper reflects the authors' own research and analysis in a truthful and complete manner.
4) The paper properly credits the meaningful contributions of co-authors and co-researchers.
5) The results are appropriately placed in the context of prior and existing research.
6) All sources used are properly disclosed (correct citation).
7) All authors have been personally and actively involved in substantial work leading to the paper, and will take public responsibility for its content.

I agree with the above statements and declare that this submission follows the policies outlined in the Guide for Authors and in the Ethical Statement.

CRediT authorship contribution statement

Antoine Pfefer: Writing – original draft, Visualization, Validation, Software, Resources, Methodology, Investigation, Formal analysis, Data curation, Conceptualization. **Bertrand Ygorra:** Writing – original draft, Validation, Software, Methodology, Conceptualization. **Frederic Frappart:** Writing – original draft, Validation, Software, Methodology, Conceptualization. **Gabriela Demarchi:** Writing – original draft, Validation, Investigation, Formal analysis, Data curation. **Benjamin Pillot:** Software, Methodology, Conceptualization. **Julie Subervie:** Supervision, Project administration, Funding acquisition, Conceptualization. **Jean-Pierre Wigneron:** Software, Methodology, Conceptualization. **Thibault Catry:** Writing – original draft, Validation, Supervision, Resources, Project administration, Methodology, Investigation, Funding acquisition, Formal analysis, Data curation, Conceptualization.

Declaration of competing interest

The authors declare that they have no known competing financial interests or personal relationships that could have appeared to influence the work reported in this paper.

Data availability

Link to the code is shared in the manuscript

Acknowledgements

This work was funded by the University of Montpellier (MUSE program) in the frame of the Forest 4 Food project.

References

Almeida, C.A., Maurano, L.E.P., de Morisson Valeriano, D., Camara, G., Vinhas, L., Gomes, A.R., Monteiro, A.M.V., de Almeida Souza, A.A., Renno, C.D., Silva, D.E., et al., 2021. Methodology for forest monitoring used in prodes and deter projects. CEP 12.

Bouvet, A., Mermoz, S., Ballere, M., Koleck, T., Le Toan, T., 2018. Use of the sar shadowing effect for deforestation detection with sentinel-1 time series. Rem. Sens. 10, 1250. https://doi.org/10.3390/rs10081250.

Demarchi, G., Subervie, J., Catry, T., Tritsch, I., 2023. Using publicly available remote sensing products to evaluate redd+ projects in Brazil. Global Environ. Change 80. https://doi.org/10.1016/j.gloenvcha.2023.102653.

Demarchi, G., 2022. Les paiements pour services environnementaux (pse) sont-ils efficaces pour reduire la deforestation en amazonie bresilienne? INRAE Sciences Sociales 4, 2.

Doblas, J., Reis, M.S., Belluzzo, A.P., Quadros, C.B., Moraes, D.R., Almeida, C.A., Maurano, L.E., Carvalho, A.F., Sant'Anna, S.J., Shimabukuro, Y.E., 2022. Deter-r: an operational near-real time tropical forest disturbance warning system based on sentinel-1 time series analysis. Rem. Sens. 14, 3658. https://doi.org/10.3390/rs14153658.

Doblas Prieto, J., Lima, L., Mermoz, S., Bouvet, A., Reiche, J., Watanabe, M., et al., 2023. Inter-comparison of optical and SAR-based forest disturbance warning systems in the Amazon shows the potential of combined SAR-optical monitoring. Int. J. Rem. Sens. 44 (1), 59–77. https://doi.org/10.1080/01431161.2022.2157684.

Gatti, L.V., Basso, L.S., Miller, J.B., Gloor, M., Gatti Domingues, L., Cassol, H.L., Tejada, G., Aragao, L.E., Nobre, C., Peters, W., et al., 2021. Amazonia as a carbon source linked to deforestation and climate change. Nature 595, 388–393. https://doi.org/10.1038/s41586-021-03629-6.

Gibson, L., Lee, T.M., Koh, L.P., Brook, B.W., Gardner, T.A., Barlow, J., Peres, C.A., Bradshaw, C.J., Laurance, W.F., Lovejoy, T.E., et al., 2011. Primary forests are irreplaceable for sustaining tropical biodiversity. Nature 378–381. https://doi.org/10.1038/nature10425.

Godar, J., Gardner, T.A., Tizado, E.J., Pacheco, P., 2014. Actor-specific contributions to the deforestation slowdown in the brazilian amazon. Proc. Natl. Acad. Sci. USA 111, 15591–15596. https://doi.org/10.1073/pnas.1322825111.

Hansen, M.C., Potapov, P.V., Moore, R., Hancher, M., Turubanova, S.A., Tyukavina, A., Thau, D., Stehman, S.V., Goetz, S.J., Loveland, T.R., et al., 2013. High-resolution global maps of 21st-century forest cover change. Science 342, 850–853. https://doi.org/10.1126/science.1244693.

Kalamandeen, M., Gloor, E., Mitchard, E., Quincey, D., Ziv, G., Spracklen, D., Spracklen, B., Adami, M., Aragao, L.E., Galbraith, D., 2018. Pervasive rise of small-scale deforestation in amazonia. Sci. Rep. 8, 1–10. https://doi.org/10.1038/s41598-018-19358-2.

Manogaran, G., Lopez, D., 2018. Spatial cumulative sum algorithm with big data analytics for climate change detection. Comput. Electr. Eng. 65, 207–221. https://doi.org/10.1016/j.compeleceng.2017.04.006.

Maurano, L.E.P., Escada, M.I.S., 2019. Comparacao dos dados produzidos pelo prodes versus dados do mapbiomas para o bioma amazonia, Simp. Bras. Rem. Sens. 19, 735–738.

Montero-de Oliveira, F.E., Blundo-Canto, G., Ezzine-de Blas, D., 2023. Under what conditions do payments for environmental services enable forest conservation in the amazon? a realist synthesis. Ecol. Econ. https://doi.org/10.1016/j.ecolecon.2022.107697.

Pickens, A.H., Hansen, M.C., Adusei, B., Potapov, P., 2020. Sentinel-2 Forest Loss Alert. Global Land Analysis and Discovery (GLAD). University of Maryland.

Reiche, J., Mullissa, A., Slagter, B., Gou, Y., Tsendbazar, N.-E., Odongo-Braun, C., Vollrath, A., Weisse, M.J., Stolle, F., Pickens, A., et al., 2021. Forest disturbance alerts for the Congo basin using sentinel 1. Environ. Res. Lett. 16. https://doi.org/10.1088/1748-9326/abd0a8.

Reigber, A.G., Martin del Campo Becerra, Jager, M., 2019. Pyrat: A Flexible Sar Postprocessing Toolbox in ESA POLinSAR Workshop.

Roopsind, A., Sohngen, B., Brandt, J., 2019. Evidence that a national redd+ program reduces tree cover loss and carbon emissions in a high forest cover, low deforestation country. Proc. Natl. Acad. Sci. USA 116, 24492–24499. https://doi.org/10.1073/pnas.1904027116.

Roy, S., O'Shea, T., Bishop, C., Stone, N., Curdoglo, M., Pandey, P., et al., 2021. High-res for tropical forests: the NICFI data program. AGU Fall Meeting Abstracts 2021. . GC43D-01.

ScienceForAmazonas, 2022. Sentinel 1 for Science Amazonas. https://senama.gisat.cz// (Accessed 25 April 2023).

Sills, E.O., Atmadja, S.S., de Sassi, C., Duchelle, A.E., Kweka, D.L., Resosudarmo, I.A.P., Sunderlin, W.D. (Eds.), 2014, REDD+ on the Ground: A Case Book of Subnational Initiatives across the Globe. Cifor.

Simonet, G., Karsenty, A., Newton, P., de Perthuis, C., Schaap, B., Seyller, C., 2015. REDD+ projects in 2014: An overview based on a new database and typology (Les Cahiers de La Chaire Economie Du Climat). Chaire Economie du Climat, Information and debates Series vol. 32, 34.

Souza, C., Azevedo, T., 2017. Mapbiomas general handbook. MapBiomas: Sao Paulo, Brazil 1–23. https://doi.org/10.13140/RG.2.2.31958.88644.

Torres, R., Snoeij, P., Geudtner, D., Bibby, D., Davidson, M., Attema, E., Potin, P., Rommen, B., Floury, N., Brown, M., et al., 2012. Gmes sentinel-1 mission. Remote Sens. Environ. 120, 9–24. https://doi.org/10.1016/j.rse.2011.05.028.

Trancoso, R., 2021. Changing amazon deforestation patterns: urgent need to restore command and control policies and market interventions. Environ. Res. Lett. 16. https://doi.org/10.1088/1748-9326/abee4c.

Truckenbrodt, J., Cremer, F., Baris, I., Eberle, J., et al., 2019. Pyrosar: framework for large-scale sar satellite data processing. In: Proceedings of the Big Data from Space, Munich, Germany. pp. 19–20. https://doi.org/10.13140/RG.2.2.16424.83206.

Tyukavina, A., Hansen, M.C., Potapov, P., Parker, D., Okpa, C., Stehman, S.V., Kommareddy, I., Turubanova, S., 2018. Congo basin forest loss dominated by increasing smallholder clearing. Sci. Adv. 4. https://doi.org/10.1126/sciadv.aat2993.

Vancutsem, Achard, C.F., Pekel, J.-F., Vieilledent, G., Carboni, S., Simonetti, D., Gallego, J., Aragao, L.E., Nasi, R., 2021. Long-term (1990–2019) monitoring of forest cover changes in the humid tropics. Sci. Adv. 7. https://doi.org/10.1126/sciadv.abe1603.

West, T.A., Borner, J., Sills, E.O., Kontoleon, A., 2020. Overstated carbon emission reductions from voluntary redd+ projects in the brazilian amazon. Proc. Natl. Acad. Sci. USA 117, 24188–24194. https://doi.org/10.1073/pnas.2004334117.

Ygorra, B., Frappart, F., Wigneron, J.-P., Moisy, C., Catry, T., Baup, F., Hamunyela, E., Riazanoff, S., 2021a. Monitoring loss of tropical forest cover from sentinel-1 time-series: a cusum-based approach. Int. J. Appl. Earth Obs. Geoinf. 103. https://doi.org/10.1016/j.jag.2021.102532.

Ygorra, B., Frappart, F., Wigneron, J.-P., Moisy, C., Catry, T., Baup, F., Hamunyela, E., Riazanoff, S., 2021b. Deforestation monitoring using sentinel-1 sar images in humid tropical areas. In: 2021 IEEE Int. Geosci. Remote Sens. Symp. (IGARSS). IEEE, p. 5957–855 5960. https://doi.org/10.1109/IGARSS47720.2021.9554698.

Ygorra, B., Frappart, F., Wigneron, J.-P., Catry, T., Pillot, B., Pfefer, A., Courtalon, J., Riazanoff, S., 2023. A near-real-time tropical deforestation monitoring algorithm based on cusum change detection method. Rem. Sens. submitted for publication.